Non-volcanic tremor resulting from the combined effect of Earth tide and slow slip event

Ryoko Nakata[1], Naoki Suda[1] & Hiroshi Tsuruoka[2]

[1]Department of Earth and Planetary Systems Science, Hiroshima University, Kagamiyama 1-3-1, Higashi-Hiroshima 739-8526, Japan. [2]Earthquake Research Institute, University of Tokyo, Yayoi 1-1-1, Bunkyo-ku, Tokyo 113-0032, Japan.

Swarms of non-volcanic tremor[1,2] occur with slow slip events[3] along the subduction zone of the Philippine Sea plate in southwest Japan. These episodic events are considered to be linked in a stress relaxation process at subducting plate interface[3-5]. Tremor swarms often exhibit occurrences with a periodicity of about 12 or 24 hours[6,7]. Here we show that the observed periodic tremor occurrences can be reproduced by the seismicity rate[8] calculated from the periodic stress due to Earth tide combined with the transient stress due to slow slip event. The value of fault constitutive parameter in tremor source region is very small, indicating a sensitive response of tremor occurrences to stress change. Observation of non-volcanic tremor is therefore effective for monitoring the stress relaxation process at subducting plate interface.

Recent studies have revealed that new kinds of earthquakes occur along the subduction zone of the Philippine Sea plate in southwest Japan[1-3,9,10]. These earthquakes are of non-volcanic origin, and have longer source times than ordinary earthquakes with comparable magnitudes. Their source times and magnitudes satisfy a new scaling law, so that they are categorized into "slow earthquakes"[11]. Occurrence of the slow earthquakes is explained as a stress relaxation process on fault segments in the transition zone of subducting plate interface[3-5,9,10], updip portion of which is the locked zone where megathrust earthquakes are predicted to occur in the near future. Monitoring the slow earthquakes is therefore important for assessing occurrence of the megathrust earthquakes since any stress relaxation phenomena in the transition zone will affect the stress state in the locked zone, and vice versa.

Among the slow earthquakes swarms of non-volcanic tremor (NVT) is most suitable for monitoring the stress relaxation process since they can be observed in real time and with the highest signal-to-noise ratio. In the eastern Shikoku area NVT swarms repeatedly occur at intervals of two to three months[12]. Each swarm lasts from three to ten days, and their epicentres migrate with a typical velocity of 10 km day^{-1}. Figure 1 shows distribution of epicentres of two NVT swarms that occurred in May 2005 and February 2006. Since NVTs occur intermittently without clear onsets we determined their hypocentres from continuous seismic records every two minutes by using the envelope correlation method[12]. The results for the May 2005 and February 2006 swarms indicate west- and eastward migrations, respectively. In all the areas where NVT occurs, short-term slow slip event (SSE) is observed in accordance with NVT source migration[12], suggesting that it is a manifestation of the rupture propagation of SSE.

Another characteristic of NVT swarms is that they often exhibit occurrences with a periodicity of about 12 or 24 hours, suggesting a close relationship to the Earth tide[6,7]. Figure 2 shows time sequences of hourly NVT durations that were determined by using

our detection method (Supplementary Methods 1). NVTs occur with periodicities of about 24 and 12 hours in the May 2005 and February 2006 swarms, respectively. Figure 2 also shows time series of the Coulomb failure stress (ΔCFS) and the rate of ΔCFS calculated from the theoretical solid Earth tide and ocean tide loading[13]. Assuming that NVTs occur as thrust faulting at the subducting plate interface, we calculated ΔCFS from the theoretical tidal stress evaluated at the central point of the epicentre distribution on the thrust fault plane. The dominant period of NVT occurrence is consistent with that of the Earth tide in each swarm interval, which is a strong evidence for the tidal origin. It seems that both ΔCFS and the ΔCFS rate are well correlated to the NVT occurrences. However, the NVT occurrences are advanced by a few hours relative to ΔCFS, which indicates that the simple ΔCFS threshold model is inappropriate for explaining the NVT occurrences on the basis of causality alone.

On the other hand, the NVT occurrences are delayed by a few hours relative to the ΔCFS rate. The dependence on the ΔCFS rate and the time delay of events are characteristics that can be reproduced by incorporating the rate- and state-dependent friction (R/S) law[8], which was derived from observations of laboratory fault experiments. The theory of seismicity rate based on the R/S law has been successfully applied to shallow earthquake phenomena[14,15], showing that it is a powerful tool for analysing the rate change of earthquakes. Laboratory fault experiments for the constants in the R/S law have been performed at the physical conditions relevant to source region of the slow earthquakes[16,17]. Recently, the R/S law is widely applied to occurrences of SSEs[18,19]. In this study we apply the R/S seismicity rate theory to the NVT occurrences. The seismicity rate theory predicts the relative number of earthquakes from the time history of stress changes. Assuming that the NVT duration is approximately proportional to the number of NVTs, we use the hourly NVT durations shown in Fig. 2 as the data to be compared with calculated seismicity rates. Such an approximation may

lead us to underestimate the peak values. See Supplementary Methods 2 for discussion on the effect of approximation on our final result.

A key feature of the R/S seismicity rate is that stress perturbations produce large changes in seismicity rate. Here we consider stress changes in NVT source region based on the model of concurrent slow earthquakes[9]. SSEs are slow slips of thrust fault segments in the transition zone, where the fault coupling is weaker than that in the locked zone. The other slow earthquakes are ruptures of relatively stronger patches included in the fault segment matrix. An SSE starts when accumulated tectonic stress due to the plate subduction evokes instability of the fault segment matrix. During the SSE, shear stress in the fault segment matrix decreases while increasing in the stronger patches, and eventually the relatively small patches rupture in NVTs. The stress change in NVT source region is thus composed of the secular change due to the plate subduction, the transient change due to the triggering SSE, and the periodic change due to the Earth tide. The secular stress rate would be ~0.03 kPa day^{-1}, which is obtained from a strain rate of 10^{-7} yr^{-1} (ref. 20) and a rigidity of 30 GPa. The transient stress rate can be estimated if detailed source process is obtained for short-term SSEs, but we have no reliable estimation at present.

We obtain the seismicity rate profiles that give the best fits to the observed NVT sequences. The unknown transient stress rate is expressed as a single box-car function, whose amplitude, start and end times are parameters to be determined. Another unknown is the combined parameter $A\sigma$ in the seismicity rate theory, where A is the fault constitutive constant, and σ is the effective normal stress. Using the same tidal ΔCFS rate as shown in Fig. 2 and the secular stress rate of 0.03 kPa day^{-1}, we determined these unknowns by using the simplex method in which we maximized the cross-correlation coefficient between the observed NVT sequence and the calculated seismicity rate. Figure 3 shows the resultant seismicity rate profiles compared with the

observed sequences of NVT occurrences. The periodic NVT occurrences in the swarm intervals match well with the seismicity rate profiles. Note that the non-linear dependence of seismicity rate on stress rate amplifies the effect of periodic tidal stress. This amplification is caused by the additional transient stress change. See Supplementary Methods 2 for the inversion and error analysis.

We obtained $A\sigma$ value of 1.3 kPa, which is an order of magnitude smaller than 10-30 kPa obtained for shallow earthquake swarms[15]. The combined parameter $(A\text{-}B)\sigma$ was estimated to be 600 kPa from the observation of afterslip following the 2003 Tokachi-oki earthquake[21]. Analysis of fault slip history provides $(A\text{-}B)\sigma$, but use of the seismicity rate theory allows us to obtain $A\sigma$. Since $B > 0$, the value of $(A\text{-}B)\sigma$ can be regarded as the lower limit of $A\sigma$. The present value of $A\sigma$ is therefore at least two orders of magnitude smaller than the value from the afterslip. This may represent the difference between the physical conditions on cold Pacific and hot Philippine Sea plate interfaces. The combined parameter $A\sigma$ controls the response of seismicity rate to stress changes. The smaller it is, the more sensitive is the seismicity rate response. Taking advantage of the high sensitivity of NVT occurrences, we can use NVT swarms as sensors for monitoring the stress relaxation process in the transition zone.

Laboratory experiments show that the value of A lies in between 0.005 to 0.015 (ref. 8). If we adopt 0.01 for A, the effective normal stress becomes on the order of 100 kPa. It was shown that surface waves radiated from a great earthquake triggered transient NVTs in the Cascadia subduction zone[22]. Shear stress deviation due to the surface waves was estimated to be about 40 kPa at the plate interface, which suggests a very low effective stress. NVT source regions in southwest Japan are well correlated to the region of high V_P/V_S, which is explained as high pore fluid pressure resulted from dehydration of the subducting oceanic crust[23]. The results of recent studies thus suggest

the existence of a low effective stress. The role of fluid is a key to understand occurrences of the slow earthquakes.

We obtained the transient stress rate of 4~6 kPa day^{-1}, which is comparable to the tidal stress rate. If the transient stress rate is substantially smaller than the tidal stress rate, NVTs will not be triggered. Also, if it is quite large, the periodic occurrence will not be observed. A typical stress drop of short-term SSEs is roughly estimated to be ~10 kPa (ref. 11). Dividing this value by a typical SSE duration of several days yields a stress rate on the order of 1 kPa day^{-1}, which is consistent with the present result.

Besides the two swarms shown above, we have analyzed the other major NVT swarms that occurred in the eastern Shikoku area during 2004 to mid-2007. Out of the total of 13 major swarms, 12 can be explained by calculated seismicity rates (Supplementary Fig. S1). Therefore, we can safely say that the tidal synchronicity is a normal feature in the eastern Shikoku area. We are now analyzing swarms in the western Shikoku area, and tentative results show that some of the swarms are not correlated with the Earth tide. To synchronize NVT occurrences with the Earth tide, the rate of transient stress needs to be comparable to that of the tidal stress. If the former is significantly larger than the latter, non-periodic, burst occurrences will dominate. Short-term SSEs have often been clearly observed in the western area compared with those in the eastern area[12]. The stress rate due to SSEs in the western area may be generally larger than that in the eastern area. We require further analyses to elucidate regional characteristics of NVT occurrences in southwest Japan.

1. Obara, K. Nonvolcanic deep tremor associated with subduction in southwest Japan. *Science* **296,** 1679–1681 (2002).

2. Katsumata, A. & Kamaya, N. Low-frequency continuous tremor around the Moho discontinuity away from volcanoes in the southwest Japan. *Geophys. Res. Lett.* **30,** doi:10.1029/2002GL015981 (2003).

3. Obara, K., Hirose, H., Yamamizu, F. & Kasahara, K. Episodic slow slip events accompanied by non-volcanic tremors in southwest Japan subduction zone. *Geophys. Res. Lett.* **31,** doi:10.1029/2004GL020848 (2004).

4. Shelly, D. R., Beroza, G. C., Ide, S. & Nakamula, S. Low-frequency earthquakes in Shikoku, Japan, and their relationship to episodic tremor and slip. *Nature* **442,** 188–191 (2006).

5. Shelly, D. R., Beroza, G. C. & Ide, S. Non-volcanic tremor and low-frequency earthquake swarms. *Nature* **446,** 305–307 (2007).

6. Shelly, D. R., Beroza, G. C.& Ide, S. Complex evolution of transient slip derived from precise tremor locations in western Shikoku, Japan. *Geochem. Geophys. Geosyst*. **8,** 10, Q10014, doi:10.1029/2007GC001640 (2007).

7. Rubinstein, J. L., Rocca, M. L., Vidale, J. E., Creager, K. C. & Wech, A. G. Tidal modulation of nonvolcanic tremor. *Science* **319,** 186-189 (2008).

8. Dieterich, J. A constitutive law for rate of earthquake production and its application to earthquake clustering. *J. Geophys. Res.* **99,** 2601–2618 (1994).

9. Ito, Y., Obara, K., Shiomi, K., Sekine, S. & Hirose, H. Slow earthquakes coincident with episodic tremors and slow slip events. *Science* **315,** 503–506 (2007).

10. Ide, S., Imanishi, K., Yoshida, Y., Beroza, G. C. & Shelly, D. R. Bridging the gap between seismically and geodetically detected slow earthquakes. *Geophys. Res. Lett.* **35,** doi:10.1029/2008GL034014 (2008).

11. Ide, S., Beroza, G. C., Shelly, D. R. & Uchide, T. A scaling law for slow earthquakes. *Nature* **447,** 76-79 (2007).

12. Obara, K. & Hirose, H. Non-volcanic deep low-frequency tremors accompanying slow slips in the southwest Japan subduction zone. *Tectonophysics* **417,** 33-51 (2006).

13. Tsuruoka, H., Ohtake, M. & Sato, H., Statistical test of the tidal triggering of earthquakes: contribution of the ocean tide loading effect. *Geophys. J. Int.* **122,** 183-194 (1995).

14. Dieterich, J., Cayol, V. & Okubo, P. The use of earthquake rate changes as a stress meter at Kilauea volcano. *Nature* **408,** 457–460 (2000).

15. Toda, S., Stein, R. S. & Sagiya, T. Evidence from the AD 2000 Izu islands earthquake swarm that stressing rate governs seismicity. *Nature* **419,** 58–61 (2002).

16. Chester, F. M. & Higgs, N. G. Multimechanism friction constitutive model for ultrafine quartz gouge ay hypocentral conditions. *J. Geophys. Res*. **97,** 1859-1870 (1992).

17. Blanpied, M. L., Marone, C. J., Lockner, D. A., Byerlee, J. D. & King, D. P. Quantitative measure of the variation in fault rheology due to fluid-rock interactions. *J. Geophys. Res.* **103,** B5, 9691-9712 (1998).

18. Kodaira, S. et al. High pore fluid pressure may cause silent slip in the Nankai trough. *Science* **304,** 1295-1298 (2004).

19. Shibazaki, B. & Shimamoto, T. Modelling of short-interval silent slip events in deeper subduction interfaces considering the frictional properties at the unstable-

stable transition regime. *Geophys. J. Int.* doi:10.1111/j.1365-246X.2007.03434.x (2007).

20. Sagiya, T., Miyazaki, S. & Tada, T. Continuous GPS array and present-day crustal deformation of Japan. *Pure Appl. Geophys.* **157,** 2303–2322 (2000).

21. Miyazaki, S., Segall, P., Fukuda, J., & Kato, T. Space time distribution of afterslip following the 2003 Tokachi-oki earthquake: Implications for variations in fault zone frictional properties. *Geophys. Res. Lett*. **31,** doi:10.1029/2003GL019410 (2004).

22. Rubinstein, J. L. et al. Non-volcanic tremor driven by large transient shear stresses. *Nature* **448,** 579-582 (2007).

23. Matsubara, M., Obara, K. & Kasahara, K. High-V_P/V_S zone accompanying non-volcanic tremors and slow slip events beneath southwestern Japan. *Tectonophysics*, doi: 10.1016/j.tecto.2008.06.013 (2008).

Figure 1 | Distribution of Epicentres of NVT swarms. a, NVT epicentres of the May 2005 swarm (circle), seismic stations (triangle), and the point at which theoretical tidal stress was evaluated (square). Epicentre colours represent origin times (see colour scale below). NVT hypocentres were determined by analysing vertical component records from 14 seismic stations of Hi-net, Kyoto and Kochi Universities. The red box in the inset shows the eastern Shikoku area. PA, Pacific plate; PS, Philippine Sea plate; AM, Amur plate; OK, Okhotsk plate. b, Same as a but for the February 2006 swarm.

Figure 2 | Comparison of observed NVT occurrences and theoretical tidal Coulomb failure stress. a, Time sequence of hourly NVT durations for the May 2005 swarm (bars), time series of the rate of ΔCFS (solid line) and ΔCFS (broken line) due to the Earth tide. The left vertical axes indicate ΔCFS and the ΔCFS rate, and the right axis indicates the hourly NVT durations. b, Same as a but for the February 2006 swarm.

Figure 3 | Comparison of calculated seismicity rate and observed NVT occurrences. a, Time series of the seismicity rate (solid line) and time sequence of the hourly NVT durations for the May 2005 swarm (bars). The left and right vertical axes indicate the seismicity rate and hourly NVT durations, respectively. The dotted box-car indicates the additional transient stress. b, Same as a but for the February 2006 swarm.

Supplementary Information is linked to the online version of the paper at www.nature.com/nature.

Acknowledgements We thank Y. Fukao, K. Shimazaki and T. Shimamoto for comments. This work was supported by a Grant-in-Aid for Scientific Research, the Ministry of Education, Sports, Science and Technology, Japan (to N.S.).

Author contributions R. N. performed the inversion based on the seismicity rate theory. N. S. developed the tremor detecting method and supervised the whole research. H. T. calculated the theoretical tidal stress.

Author Information Reprints and permissions information is available at http://npg..nature.com/reprintsandpermissions. The authors declare no competing financial interests. Correspondence and requests for materials should be addressed to R. N. (nakata@geol.sci.hiroshima-u.ac.jp).

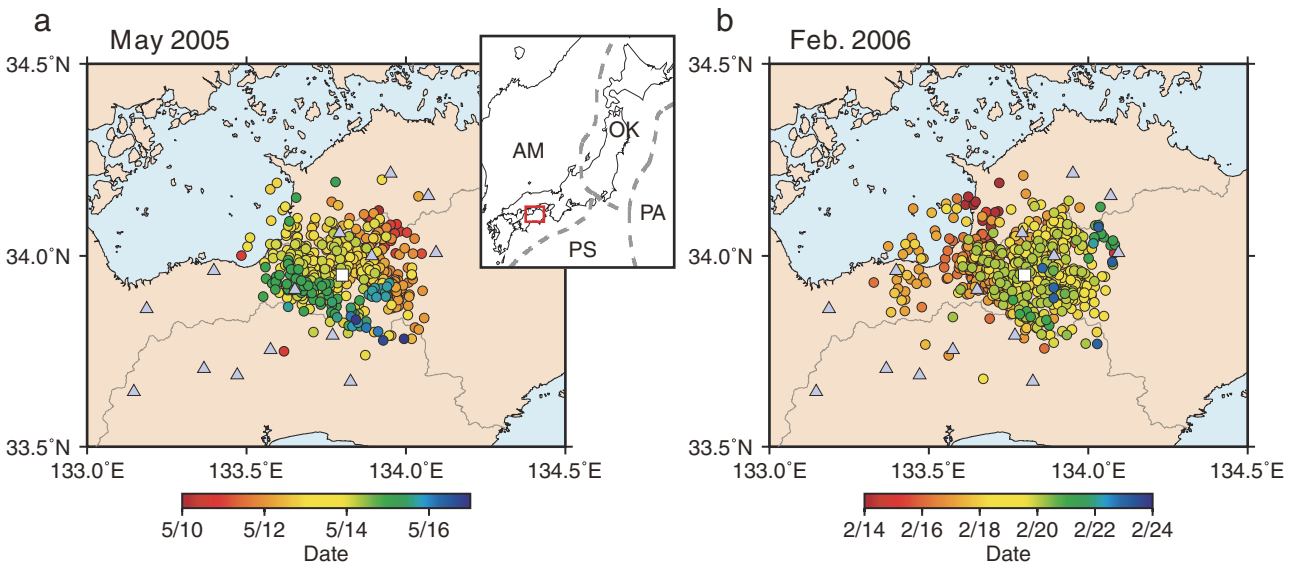
a
May 2005
34.5˚N
34.0˚N
33.5˚N
133.0˚E
133.5˚E
134.0˚E
134.5˚E
AM
OK
PA
PS
5/10
5/12
5/14
5/16
Date
b
Feb. 2006
34.5˚N
34.0˚N
33.5˚N
133.0˚E
133.5˚E
134.0˚E
134.5˚E
2/14
2/16
2/18
2/20
2/22
2/24
Date

Nakata, Fig. 1

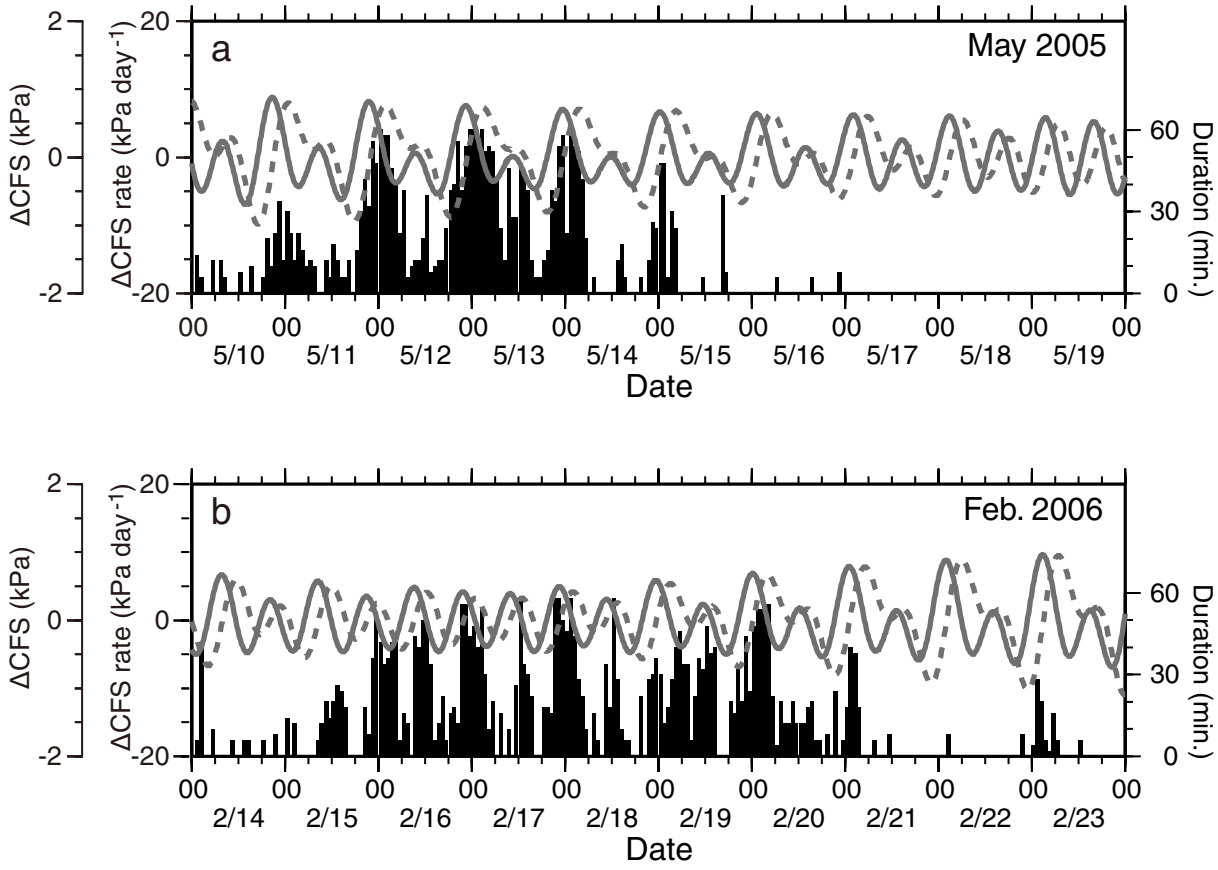
a
May 2005
ΔCFS (kPa)
ΔCFS rate (kPa day-1)
Duration (min.)
2
0
-2
20
0
-20
60
30
0
00
5/10
5/11
5/12
5/13
5/14
5/15
5/16
5/17
5/18
5/19
Date
b
Feb. 2006
2/14
2/15
2/16
2/17
2/18
2/19
2/20
2/21
2/22
2/23

Nakata, Fig. 2

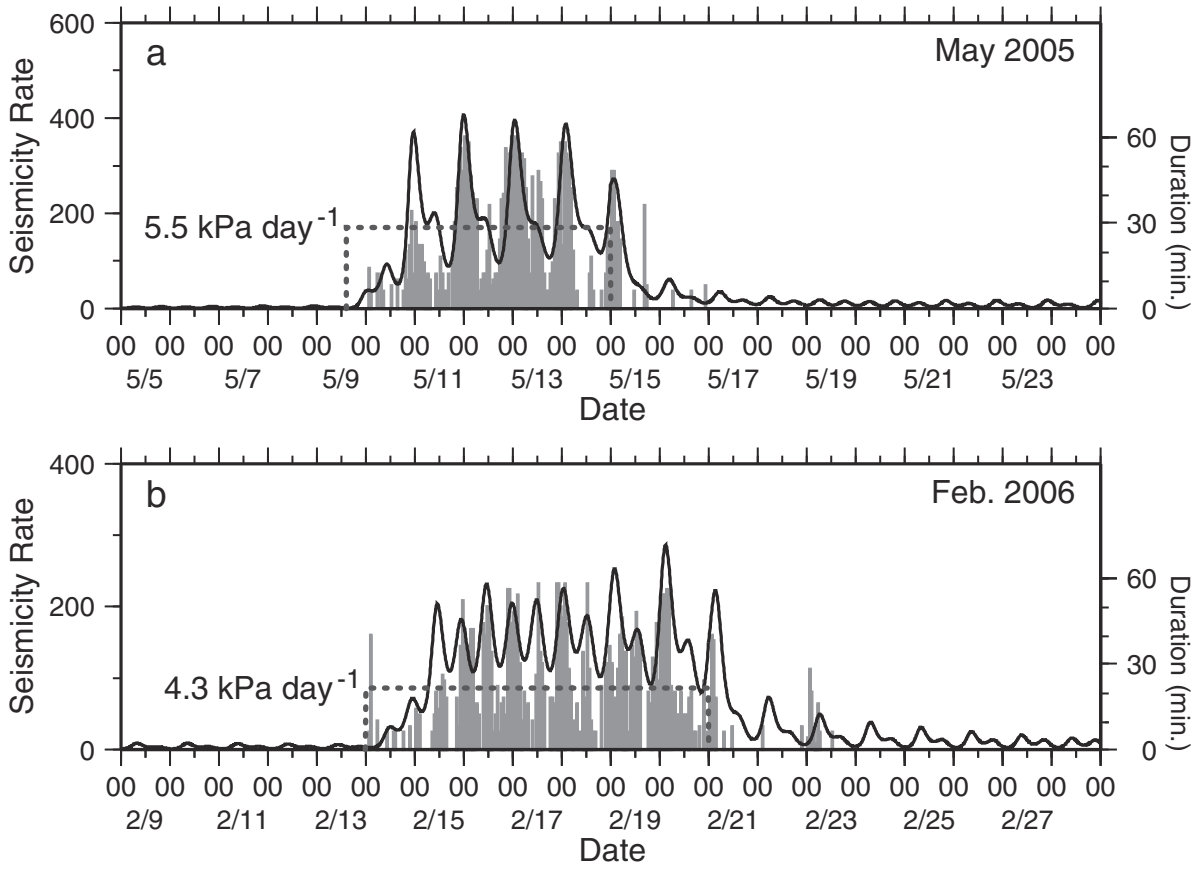
a
May 2005
5.5 kPa day-1
Seismicity Rate
Duration (min.)
Date
b
Feb. 2006
4.3 kPa day-1
Seismicity Rate
Duration (min.)
Date

Nakata, Fig. 3

Supplementary Figures and Legends 1:

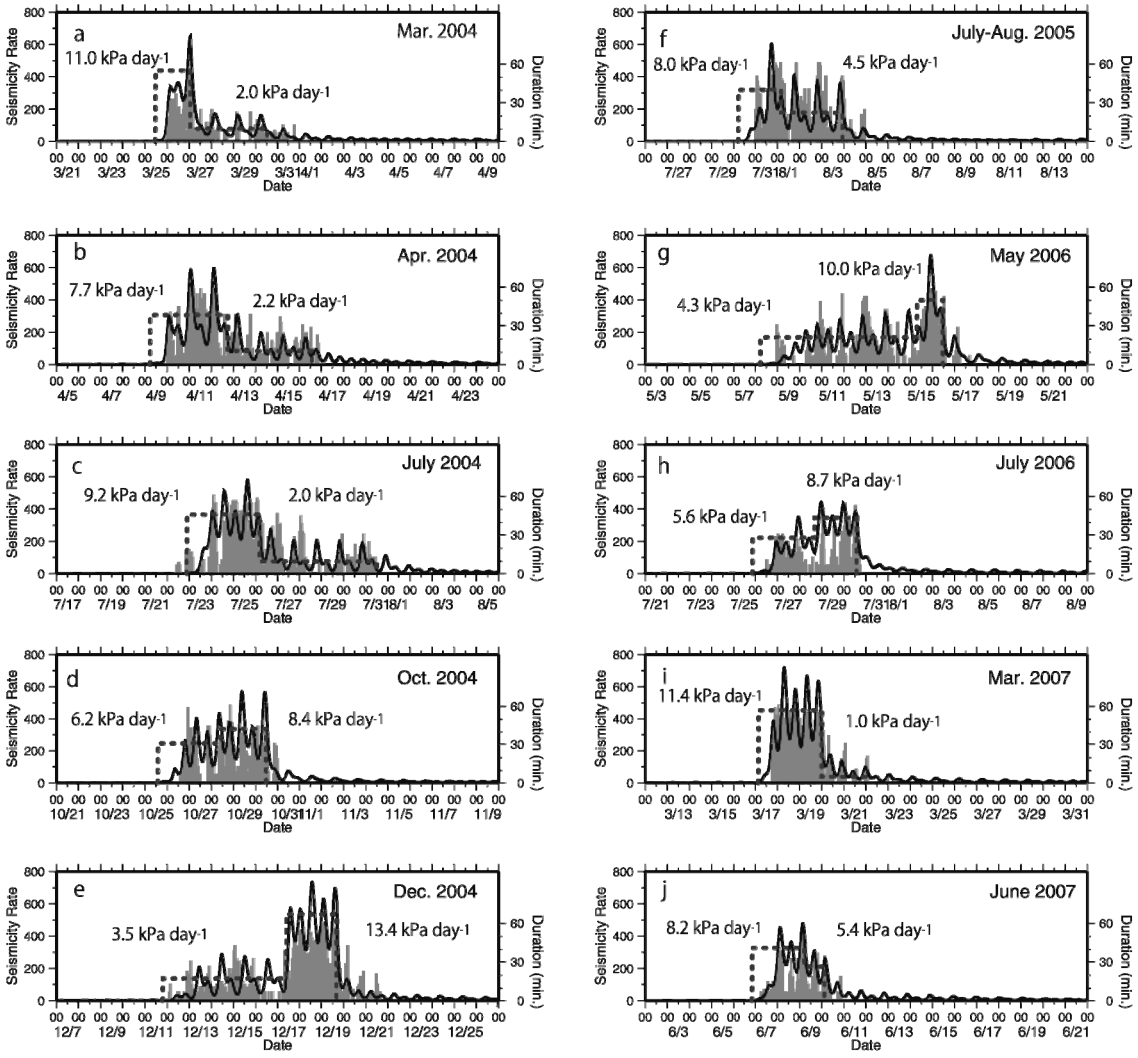

Figure S1 | Comparison of calculated seismicity rate and observed NVT occurrences for the other major swarms. Same as Fig. 3 but for the other major NVT swarms in the eastern Shikoku area during 2004 to mid-2007. The seismicity rate profiles were determined by the same method as in the main text, but we expressed the transient stress rate as two connected box-car functions since activities of these swarms were not as monotonous as the two swarms shown in Fig. 3. In the calculations we fixed the value of $A\sigma$ as 1.3 kPa.

Supplementary Methods 1:

We search for NVT occurrences by applying a detection method based on a statistical hypothesis test to continuous vertical-component seismograms every two minutes. Before applying the detection method, we process raw seismograms as follows: (1) removing the linear trend and bandpass filtering between 2 and 10 Hz, (2) resampling the data points from 100 Hz to 20 Hz, (3) calculating the envelope and applying the moving-average with a time window of 3 seconds. We apply a two-step statistical hypothesis test to the resultant envelope seismograms. The null hypotheses are "no correlation between given two seismograms" and "no event in given two minutes", and the test statistics are maximum cross-correlation coefficients (MCCs) and the number of correlated seismogram combinations for the first and second tests, respectively. This two-step test is similar to the method of Beroza and Jordan[24] for detecting Earth's free oscillations, but in our method the p-values are numerically calculated as

$$p = \#\left\{ t^* \geq t_{\mathrm{obs}} \right\} / N \qquad (1)$$

where t^* is a simulated value under the null hypothesis, t_{obs} is an observed test statistic, and N is the number of simulations.

In the first test, we calculate MCCs for all the combinations of envelope seismograms, and estimate their p-values by using the bootstrap method. We obtain replications of the observed envelope seismograms using the moving-blocks bootstrap method[25], and then calculate MCCs from the replicated envelope seismograms. A total of 12 data blocks, each of which has a length of 10 seconds, are randomly sampled from an observed envelope seismogram before the moving-average procedure. The sampled blocks are then connected and moving-averaged to create a bootstrap replication. In the above procedure the blocks are allowed to be overlapped in the original seismogram. The optimal block length can be determined by the method of Davison and Hinkley[26], which provides 10-12 seconds in our case. We obtain a total of 200 simulated MCCs for each seismogram combinations to estimate the p-value using equation (1). If the p-value

is smaller than or equal to the significance level of 1 %, we reject the null hypothesis, or we judge that given two envelope seismograms are correlated. We test all the combinations of envelope seismograms, and obtain the number of correlated seismogram combinations, which is used as the test statistic in the second test.

In the second test, we estimate the p-value for the number of correlated seismogram combinations using the Monte Carlo method. Here we define the function $I(x, p_i)$ ($0 \leq x \leq 1$) as

$$I(x, p_i) = \begin{cases} 1 & (x \leq p_i) \\ 0 & (x > p_i) \end{cases} \tag{2}$$

where p_i is the observed p-value of the i-th seismogram combination obtained in the first step. We generate a normalized uniform random number x and substitute it in equation (2) to calculate $\Sigma_i I(x, p_i)$. This is a simulated value of the number of correlated seismogram combinations under the null hypothesis. We obtain a total of 2,000 simulated values to estimate the p-value using equation (1). If the p-value is smaller than or equal to the significance level of 0.1 %, we reject the null hypothesis, or we judge that an event occurs in given two minutes.

The above method detects ordinary earthquakes other than NVTs. We calculate a station average of maximum amplitudes and that of maximum STA/LTA (short time = 3 s and long time = 15 s) from the two-minute envelope seismograms. If the former is larger than 200 nm s^{-1} or the latter is larger than 3, we reject the detected event as an ordinary earthquake. Also we reject the detection if it follows an ordinary earthquake and also if the average amplitude is larger than twice that before the earthquake. After these rejections, we judge that NVTs occur if events are detected at least in three successive units of analysis, that is, for six minutes.

Critical parameters in the two-step test are the significance levels and the length of moving average window. We use the above values since they provide results that are most consistent with those from the visual inspections of waveforms. The present method can be applied to real-time seismic data distributed on high-speed networks in

Japan. We have developed an automatic monitoring system for NVTs using the present method, details of which will be published elsewhere.

Supplementary References:

24. Beroza, G. C. & Jordan, T. H., Searching for slow and silent earthquakes using free oscillations. *J. Geophys. Res.* **95**, 2485– 2510 (1990).

25. Efron, B. & Tibshirani, R. J., *An Introduction to the Bootstrap* (Chapman & Hall, New York, 1993).

26. Davison, A. C. & Hinkley, D. V., *Bootstrap Methods and Their Application* (Cambridge Univ. Press, Cambridge, 1997).

Supplementary Methods 2:

We use discretised versions of equations (1) and (2) in ref. 14 for the numerical calculations of seismicity rate. Seismicity rate relative to the reference state is expressed as

$$R_n = \frac{1}{\gamma_n \dot{S}_r} \quad (n = 0,1,2\cdots) \tag{1}$$

where γ_n is the state variable and the constant $\dot{S}_r$ is the reference Coulomb stress rate. Increment of the state variable is expressed as

$$\Delta\gamma_n = \frac{1}{A\sigma}\left(\Delta t - \gamma_{n-1}\Delta S_{n-1}\right) \quad \text{and} \quad \Delta S_n = \Delta\tau_n - [\mu - \alpha]\Delta\sigma_n \tag{2}$$

where the constant A is the dimensionless fault constitutive parameter, σ is the normal stress, Δt is the increment of time, and ΔS_n is the increment of modified Coulomb stress. Assuming that changes in σ is negligible relative to total σ, we treat $A\sigma$ as a constant. The increment of normal stress $\Delta\sigma_n$ is calculated from the theoretical tidal stress, while that of shear stress $\Delta\tau_n$ is calculated from the theoretical tidal shear stress, the secular shear stress rate of 0.03 kPa day^{-1}, and the transient shear stress rate during the triggering SSE. The constants μ and α are the coefficient of fault friction and a fault constitutive parameter, respectively, and we assign -0.2 to μ–α in this study.

Our inversion is to obtain the four unknowns: $A\sigma$, amplitude, start and end times of a box-car function representing the transient shear stress rate due to the triggering SSE. They are determined by using the simplex method in which we maximize the cross-correlation coefficient between the observed NVT sequence and the calculated seismicity rate. We obtained the $A\sigma$ value of 1.3 ± 0.1 kPa and the transient stress rate of 5.5 ± 0.9 kPa day^{-1} for the May 2005 swarm, and the respective values for the February 2006 swarm were 1.3 ± 0.1 kPa and 4.3 ± 0.4 kPa day^{-1}. The standard errors were obtained by using the parametric bootstrap method[25] in which we assumed Gaussian errors with 1σ = 6 minutes for the hourly NVT duration data. Changes in μ-α of ±0.1 resulted in changes in seismicity rate amplitude of about ±25 %, but such

changes provided almost no effect on the present result.

We used the hourly NVT durations as the data to be compared with calculated seismicity rates. Such an approximation may lead us to underestimate the peak data values since the maximum is limited to be 60 minutes. To evaluate the effect of data underestimation at activity maxima on the present result, we performed the simulated inversions in which we added extra values randomly obtained from the truncated Gaussian distribution with 1σ = 60 minutes to the data with a value of 58 or 60 minutes (the unit of our data is 2 minutes). From results of a total of 200 simulations we obtained the $A\sigma$ value of 0.9 ± 0.1 kPa and the transient stress rate of 5.2 ± 1.6 kPa day^{-1} for the May 2005 swarm, and the respective values for the February 2006 swarm were 1.0 ± 0.2 kPa and 4.4 ± 1.5 kPa day^{-1}. This shows that our final results are not significantly affected even if the data values at activity maxima are underestimated.